

# ODMTCNet: An Interpretable Multi-view Deep Neural Network Architecture for Image Feature Representation

Lei Gao, *Member, IEEE*, Zheng Guo, and Ling Guan, *Fellow, IEEE*

## Abstract

Recently, deep cascade architecture-based algorithms have attracted wide interest and have been applied to various application domains successfully. However, the longstanding challenge of interpretability, is still considered as an Achilles' heel of such algorithms. Moreover, due to its data-driven nature, the deep cascade architecture likely causes over-fitting problems when there is no sufficient data available. To address these pressing issues, this work proposes an interpretable multi-view deep neural network architecture, namely optimal discriminant multi-view tensor convolutional network (ODMTCNet), by integrating statistical machine learning (SML) principles with the deep neural network (DNN) architecture. Benefiting from the joint strength of SML and DNN, we demonstrate that ODMTCNet is analytically interpretable for multi-view image feature representation. Specifically, a discriminant multi-view tensor convolution strategy is proposed and integrated with the desired deep cascade architecture to generate high quality feature representations. Different from the traditional DNN models, the parameters of the convolutional layers in ODMTCNet are determined by analytically solving a SML-based optimization problem in each convolutional layer independently. This work demonstrates that, in ODMTCNet, the relation between the optimal performance and parameters (e.g., the number of convolutional filters) can be predicted, with each layer generating justified knowledge representations, leading to an interpretable multi-view based convolutional network. In addition, an information theoretic based descriptor, information quality (IQ), is utilized for feature representation of the given multi-view data sets. Because of its unique design, ODMTCNet is able to handle image data sets of different scales, large or small, effectively addressing the data hungry nature of DNN in image representation and forming a generic platform for multi-view image feature representation. To validate the effectiveness and the generic nature of the proposed ODMTCNet, we conducted experiments on four image data sets of different scales: The Olivetti Research Lab (ORL) database, Facial Recognition Technology (FERET) database, ETH-80 database and Caltech 256 database. The results show the superiority of the proposed solution compared to state-of-the-art.

## Index Terms

multi-view tensor convolutional network, optimal discriminant deep-level representation, interpretable DNN architecture, information quality.

## I. INTRODUCTION

With the advancement of large scale data-based techniques (e.g., big data, deep learning, etc.), there has come urgent demand to better understand and reveal the intrinsic properties of data structure in order to effectively explore useful information from massive sets of data. As a solution to this challenge, feature representation has been attracting widespread attention and investigation [1-3]. In general, the main streams of feature representation are divided into three different categories: handcrafted feature representation, prior knowledge-based feature representation and learned deep-level feature representation. In what follows, the three different categories of feature representation are introduced briefly.

Due to its ability to extract geometry and texture characteristics of given samples reliably (such as local binary pattern, scale-invariant feature transforms and gradient orientation histogram, etc.), handcrafted feature representation methodology has drawn tremendous interest and has been utilized in a variety of real applications. However, suffering from the intra-class modifiability problem [4], handcrafted methodology is difficult to perform well on unseen samples. To tackle this problem, prior knowledge-based feature representation solutions have been proposed and investigated extensively, such as manifold representation [5], subspace representation [6] and dictionary representation [7], etc. Generally, according to certain prior knowledge, the studied distinct information from given samples can be applied to new or unseen samples successfully, leading to better performance. It should be noted that, although more efforts have been committed to the development of prior knowledge-based feature representation algorithms, plenty of room is still available for further improvement, especially when working with large scale data sets [84-86].

In recent years, by generating learned deep-level feature representation, deep neural network (DNN)-based algorithms have opened up a new frontier to promote state-of-the-art in visual computing, image classification and many other computer vision tasks [8-10]. Compared with the handcrafted and prior knowledge-based feature representation strategies, deep-level feature representation attempts to mimic the workings of the human brain in processing data/information. In general, deep-level feature representation is generated by utilizing a multi-layer cascade architecture and the learning process needs enormous data samples

to guarantee that the parameters in the deep layers are tuned properly. Particularly, there are two outstanding issues, among others, with the current deep learning architectures: (a) Model interpretability, a persistent challenge since the inception of DNN research; (b) Over-fitting in the learned deep-level feature representation when there is no sufficient data available due to DNNs' data-driven nature.

One recently proposed solution to model interpretability is to modify a DNN model so that each convolutional layer generates knowledge representations, such as the loss method presented in [91] and an interpretable feedforward (FF) solution in [92]. In addition, the integration of prior knowledge with DNN-based architectures is becoming an increasingly popular research area for tackling the model interpretability problem (e.g., PCANet [11], DCTNet [12], etc.). Amongst these solutions, the model parameters are usually calculated by a certain prior knowledge-based function while the final outputs are generated by the deep cascade architecture.

On the other hand, to address the over-fitting problems in DNN-based models, the multi-view feature representation solutions have attracted enormous attention. [13] explores the integration of multi-view features for better data augmentation to tackle small sample size (SSS) problems, and yields improved performance. The study in [13] suggests that one desirable solution to balancing the small scale and deep-level feature representation is to smartly utilize multi-view features and the deep cascade structure. A canonical correlation analysis network (CCANet) is presented in [4]. CCANet can obtain more comprehensive information from the inputs, resulting in enhanced performance. However, due to its unsupervised nature, CCANet lacks the power to extract discriminant information of high quality, leading to suboptimal performance. To address this problem, a discriminative canonical correlation network (DCCNet) [14] is introduced. However, in the DCCNet, only between-class and within-class scatter matrices are employed. Since the purpose of the scatter matrices is simply to reveal and extract discriminant representations of the given samples from a single data set, such a matrix is incapable of gaining the discriminant information across different sets of features adequately. Therefore, DCCNet essentially cannot be applied to multi-view feature representation directly.

In this paper, an interpretable multi-view deep learning architecture, namely optimal discriminant multi-view tensor convolutional network (ODMTCNet), is proposed to address the model interpretability and over-fitting problems jointly. ODMTCNet is essentially based on the integration of statistical machine learning (SML) principles with DNN architecture. Specifically, in ODMTCNet, a discriminant multi-view tensor convolutional strategy is proposed and applied to the multi-view data sources. In addition, correlation matrices instead of scatter matrices are utilized and optimized to explore the discriminant information across different data sets. Note that, unlike the scatter matrices, the power of which is to reveal the discriminant relation among various samples in a single data set, the correlation matrices are capable of exploring the discriminant information across multiple data sets. Thus, the correlation matrices can more adequately explore the discriminant and intrinsic relation amongst different data sets in multi-view feature representation. In other words, the proposed ODMTCNet potentially generates a high quality feature representation for image based applications. The difference between scatter matrices and correlation matrices is depicted graphically in Figure. 1.

Since there is no loss function with given/fixed values associated with ODMTCNet, the popular backpropagation (BP) algorithm is not used in this work and the parameters of the convolutional layers in the network are determined by analytically solving a SML-based optimization problem in each convolutional layer independently instead. Moreover, according to SML principles, the relation between the optimal performance and parameters (e.g., the number of convolutional filters in each layer) in ODMTCNet is predicted analytically, providing a simple and appealing alternative to the popular try-and-error practice in DNN architecture design. Hence, each convolutional layer in the ODMTCNet model generates justified knowledge representations, making the proposed model interpretable.

In addition, by utilizing the designed discriminant multi-view tensor convolution, ODMTCNet yields more distinct multi-view feature maps for data augmentation, providing a solution for improving performance on small scale data sets. Due to the characteristics of the deep cascade architecture, ODMTCNet can also exploit abstract semantics from the large scale data sources, and therefore works well on large-scale sets as well. Finally, an information theoretic based descriptor, information quality (IQ) is introduced to generate the high quality feature representation from the original multi-view data sources. To validate the effectiveness and generality of the proposed network, we conduct experiments on four image data sets of different scales: the Olivetti Research Lab (ORL) database, Facial Recognition Technology (FERET) database, ETH-80 database and Caltech 256 database. Experimental results show the superiority of ODMTCNet over state-of-the-art for multi-view feature representation.

This paper is organized as follows: A review of related work is given in Section 2. The proposed ODMTCNet is presented in Section 3. Experiments, comparison with state-of-the-art and discussions are conducted in Section 4. Section 5 draws the conclusions.

## II. RELATED WORK

In this section, we briefly present related work on convolutional neural networks (CNN), traditional correlation analysis (TCA) and discriminant correlation analysis (DCA) methods, laying theoretical foundations for the proposed ODMTCNet.

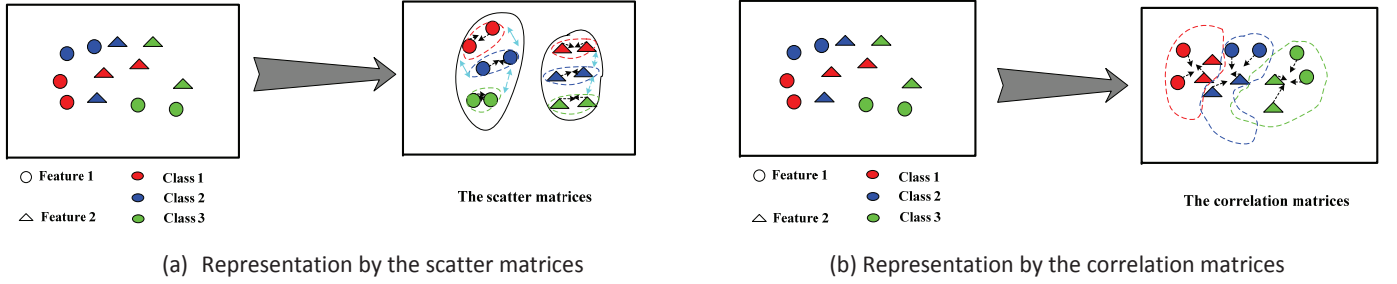


Figure. 1 The representation by scatter matrices and correlation matrices.

### A. CNN

Motivated by biological processes of the human visual cortex, CNN is proposed and applied to visual computing, video processing, image classification, among others. A typical CNN architecture usually includes convolution layers, pooling layers and fully connected layers as drawn in Figure. 2.

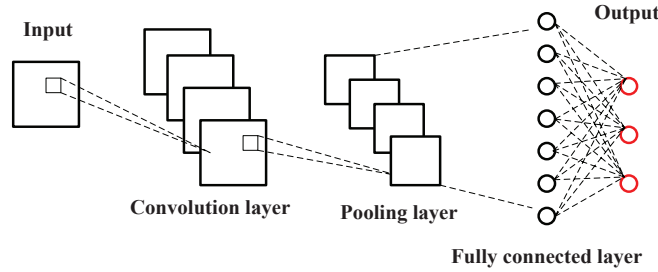


Figure. 2 A typical CNN architecture

Generally, the feedforward and backpropagation algorithms are utilized in CNN to adjust the internal parameters to reduce the targeted loss function, resulting in better performance. As the number of layers increases, enormous data samples are required to guarantee that the parameters in different layers are tuned properly for the intended tasks. Thus, a CNN is unlikely to produce satisfactory results with small scale inputs.

### B. TCA

TCA aims to find projected vectors for the given data sets to obtain the maximum correlation. Assume there are two data sets  $x$  and  $y$ . Then, the objective of TCA is to seek a pair of projected vectors  $\omega_x$  and  $\omega_y$  with the maximum correlation. Or mathematically, TCA solves the following optimization problem

$$\arg \max_{\omega_x, \omega_y} \omega_x^T R_{xy} \omega_y, \quad (1)$$

$$s.t \quad \omega_x^T R_{xx} \omega_x = \omega_y^T R_{yy} \omega_y = 1, \quad (2)$$

where  $R_{xy} = xy^T$ ,  $R_{xx} = xx^T$  and  $R_{yy} = yy^T$ . The solutions to equations (1) and (2) are gained by the eigenvalue decomposition or singular value decomposition. Nevertheless, due to the unsupervised nature, it usually leads to an unsatisfying performance.

### C. DCA

Assume there are two sets of random variables  $x_1 \sim \in R^{m_1 \times N}$ ,  $x_2 \sim \in R^{m_2 \times N}$  as the entries with  $N$  being the total number of training samples, and  $m_1$  &  $m_2$  are the respective dimensionalities of the two sets. Then, the zero-mean sets of  $x_1 \sim$  and  $x_2 \sim$  are written as  $x_1 = x_1 \sim - M_{x_1}$  and  $x_2 = x_2 \sim - M_{x_2}$  with  $M_{x_1}$  and  $M_{x_2}$  being the mean matrices in equation (3)

$$M_{x_1} = \frac{1}{N} \sum_{i=1}^N x_{1i} \sim, M_{x_2} = \frac{1}{N} \sum_{i=1}^N x_{2i} \sim, \quad (3)$$

where  $x_{1i}^{\sim}$  and  $x_{2i}^{\sim}$  are the  $i$ th sample in  $x_1^{\sim}$  and  $x_2^{\sim}$ , respectively. The within-class and between-class correlation matrices of two sets  $x_1$  and  $x_2$  are expressed as  $C_{w_{x_1x_2}}$  and  $C_{b_{x_1x_2}}$ , which are formulated as  $C_{w_{x_1x_2}} = x_1 D x_2^T$  and  $C_{b_{x_1x_2}} = -x_1 D x_2^T$  [15], where

$$D = \begin{bmatrix} \left( \begin{array}{ccc} H_{n_{i1} \times n_{i1}} & \cdots & 0 \\ \vdots & H_{n_{il} \times n_{il}} & \vdots \\ 0 & \cdots & H_{n_{ic} \times n_{ic}} \end{array} \right) \end{bmatrix} \in R^{N \times N}, \quad (4)$$

and  $n_{il}$  ( $l \in [1, 2, \dots, c]$ ) is the number of samples in the  $l$ th class within the  $i$ th data set  $x_i$  and  $H_{n_{il} \times n_{il}}$  is a square matrix of size  $n_{il} \times n_{il}$  with unit values for all the elements.

DCA aims to find a pair of projected vectors  $w_1$  and  $w_2$  with the discriminant representations by utilizing the within-class and between-class correlation matrices across two data sets, and its optimization problem is formulated as below:

$$\arg \max_{w_1, w_2} \lambda = w_1^T C_{x_1x_2}^{\sim} w_2, \quad (5)$$

subject to

$$w_1^T C_{x_1x_1} w_1 = w_2^T C_{x_2x_2} w_2 = 1, \quad (6)$$

where  $C_{x_1x_2}^{\sim} = C_{w_{x_1x_2}} - C_{b_{x_1x_2}}$ ,  $C_{x_1x_1} = x_1 x_1^T$  and  $C_{x_2x_2} = x_2 x_2^T$ . Then the Lagrange multiplier method and eigenvalue decomposition (GEV) algorithm are utilized to find the solution to equation (5). Essentially, DCA is a special case of discriminative multiple canonical correlation analysis (DMCCA) when only two data sets are utilized [15]. Moreover, there exists an important property of DCA that the number of projected dimensions  $d$  associated with the global optimal performance is smaller than or equals to the number of classes,  $c$ , or mathematically [15]

$$d \leq c. \quad (7)$$

### III. THE PROPOSED ODMTCNET

The proposed ODMTCNet consists of three types of layers: DCA driven multi-view convolutional layers, hashing controlled pooling layers and fully connected layers with information quality enhancement. Essentially, the ultimate goal of ODMTCNet is to generate a novel multi-view feature representation on image data sets of different scales. In what follows, the construction and design of these layers are presented, consecutively. Afterwards, we move on to the analysis of relationship between parameters (e.g., the number of convolutional filters) and the optimal performance.

#### A. The DCA driven multi-view convolutional layer

The convolutional layer plays a vital role in the whole CNN architecture, which is accomplished by conducting the convolution operation between inputs and the pre-defined convolutional filters [16].

Given a set of images  $I = [I_1, I_2, \dots, I_M]$ , where  $M$  is the number of images, assume there are two views of this data set,  $I^{1,M} = [I_1^1, I_2^1, \dots, I_M^1]$  and  $I^{2,M} = [I_1^2, I_2^2, \dots, I_M^2]$ . Then, the sample pair from  $I^{1,M}$  and  $I^{2,M}$  is a pair of images with a size of  $p \times q$  pixels as shown in Figure. 3.

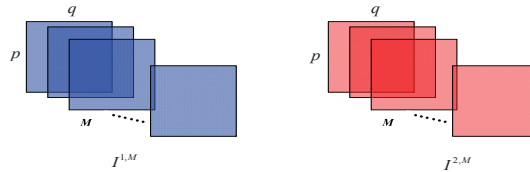


Figure. 3 Representation of two-view data sets

In Figure. 3, it is observed that  $I^{1,M}$  and  $I^{2,M}$  can be presented by two three-dimensional tensors. In the following, our target is to explore the discriminant feature representation between the two three-dimensional tensors. First, each sample pair in the given two-view data sets is divided into patches with the size of  $l_1 \times l_2$ . Next, we select an  $l_1 \times l_2$  patch around each pixel and the vectorized operation is performed on the selected patches, yielding a vector of length  $l_1 l_2$ . Thus, all patches collected from the  $k$ th sample of the  $d$ th ( $d \in [1, 2]$ ) view set are written in the vectorial forms  $I_{k,1}^d, I_{k,2}^d, \dots, I_{k,pq}^d \in R^{l_1 l_2}$ . The patches from all  $M$  samples of the  $d$ th view set are expressed as follows

$$I^d = [I_1^{d*}, I_2^{d*}, \dots, I_M^{d*}] \in R^{l_1 l_2 \times M p q}, \quad (8)$$

where

$$I_k^{d*} = [I_{k,1}^d, I_{k,2}^d, \dots, I_{k,pq}^d] \in R^{l_1 l_2 \times p q} (k \in [1, 2, \dots, M]). \quad (9)$$

In ODMTCNet, the optimization function of the DCA method is to learn the parameters of the cascade network from the input samples to explore discriminant feature representation.  $I^d$  is considered as the  $d$ th data set with size  $l_1 l_2 \times M p q$ , where  $l_1 l_2$  is the number of ‘dimensions’ and  $M p q$  is the number of ‘training samples’, respectively. As a result, the optimization function of DCA on  $I^1$  and  $I^2$  is formulated as follows

$$\arg \max_{\omega_1, \omega_2} \rho = \omega_1^T C_{I^1 I^2} \tilde{\omega}_2, \quad (10)$$

subject to

$$\omega_1^T C_{I^1 I^1} \omega_1 = \omega_2^T C_{I^2 I^2} \omega_2 = \mathbf{I}. \quad (11)$$

where  $\omega_1$  &  $\omega_2$  are projected matrices, and  $\mathbf{I}$  is an identity matrix. Based on the Lagrange multiplier method and the GEV algorithm, the solutions to  $\omega_1$  and  $\omega_2$  are of size  $l_1 l_2 \times l_1 l_2$ . Then, the corresponding column pair in  $\omega_1$  and  $\omega_2$  is chosen as one convolutional filter for the ODMTCNet model, associated with the first view and second view respectively. As a result,  $l_1 l_2$  convolutional filters are generated according to different columns in  $\omega_1$  and  $\omega_2$ . The utilization of these convolutional filters will yield  $l_1 l_2$  distinct feature maps, generating rich data augmentation which in turn enables the proposed method to improve the performance on small scale data sets. The design and construction of the convolutional filters are presented below.

Suppose we have  $L_i$  filters in the  $i$ th layer of the 1th view, the convolutional filters are formulated as below

$$W_g^1 = \text{res}_{l_1, l_2}(\omega_{1, g}) \in R^{l_1 \times l_2}, g = 1, 2, \dots, L_i (L_i < l_1 l_2), \quad (12)$$

where  $\text{res}_{l_1, l_2}(h)$  is a function to reshape  $h \in R^{l_1 l_2}$  into a matrix with size  $l_1 \times l_2$  and  $\omega_{1, g}$  is the  $g$ th column in  $\omega_1$ . Similarly, the convolutional filters in the 2th view are formulated as

$$W_g^2 = \text{res}_{l_1, l_2}(\omega_{2, g}) \in R^{l_1 \times l_2}, g = 1, 2, \dots, L_i. \quad (13)$$

Therefore, in the  $i$ th layer of the  $d$ th view, we obtain  $L_i$  feature maps  $I_{d, k, g}^{\text{out}} = \text{res}_{l_1, l_2}(I_k^{d*}) \otimes W_g^d$  from the  $k$ th sample, where ‘ $\otimes$ ’ is the 2D convolution operator. The aforementioned procedure is clearly visualized in Figure. 4.

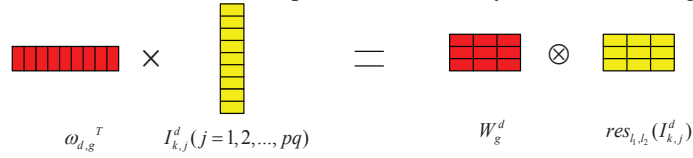


Figure 4. 2D convolution and vectors-based product operation

The above analysis shows that the feature maps from the 2D convolutional filters are generated by solving a SML-based optimization function of DCA. Since the SML-based DCA is based on mathematically/statistically solid foundation with clearly defined optimization objectives, each convolutional layer in the ODMTCNet yields and possesses justified knowledge representations. By repeating this procedure, a DNN-based cascade network is built to generate the deep-level feature representation from the two-view data sets.

### B. The pooling layer built on multi-view hashing

Based on the previous subsection, suppose there are  $L_i$  convolutional filters in the  $i$ th layer from each view and each of them corresponds to the  $L_{i+1}$  filters in the  $i+1$ th layer. Then, there are  $L_i \times L_{i+1}$  feature maps in the  $i+1$ th layer from each view. Since a cascaded network structure is employed in ODMTCNet, the total number of feature maps from convolutional filters will increase greatly with the growing of the deep network layers as depicted graphically in Figure. 5. In the figure it can be seen that, with the increase of convolutional filters and layers, the proposed ODMTCNet potentially causes a slow convergence or overfilling problem. To address this problem, a new multi-view based hashing pooling layer is utilized in this subsection.

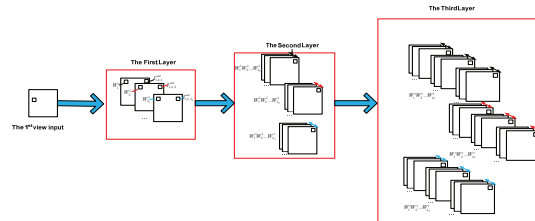


Figure 5. Relation between feature maps and layers

Essentially, the pooling layer is a specific block of a typical CNN architecture. It aims to reduce the size of the feature representation from the previous layers, leading to smaller parameters and less computation in the related networks. The popular methods include max pooling, average pooling, K-max pooling, etc. In this paper, the pooling strategy is described as follows

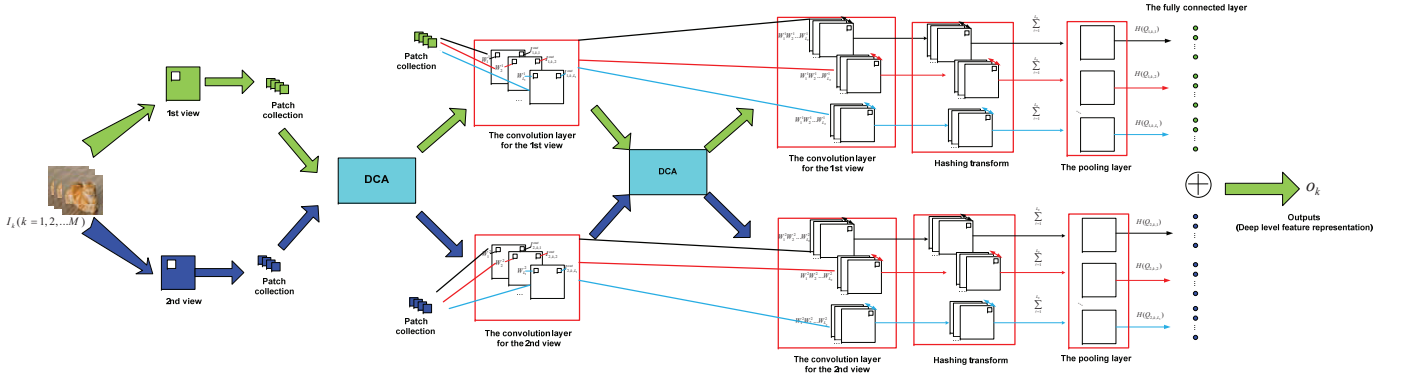


Figure. 7 The overall architecture of ODMTCNet.

[11].

Assume there are  $i + 1$  layers in the proposed ODMTCNet architecture, and the outputs are expressed as  $I_{d,k,g}^{out} \otimes W_\ell^d$  ( $\ell = 1, 2, \dots, L_{i+1}$ ) for the  $k$ th sample of the  $d$ th view, where  $I_{d,k,g}^{out}$  are the outputs of the  $i$ th layer ( $g = 1, 2, \dots, L_i$ ). Then outputs are binarized based on Hashing transform in (14)

$$S\{I_{d,k,g}^{out} \otimes W_\ell^d\} (\ell = 1, 2, \dots, L_{i+1}), \quad (14)$$

where

$$S(x) = \begin{cases} 1, & (x > 0) \\ 0, & \text{others.} \end{cases} \quad (15)$$

In essence, equation (15) can be considered as the activation function in a traditional CNN architecture. Next, the vector of  $\ell$  binary bits is considered as a decimal number, resulting in a single integer-valued “image” in (16)

$$Q_{d,k,g,\ell} = 2^{\ell-1} S\{I_{d,k,g}^{out} \otimes W_\ell^d\}. \quad (16)$$

However, since there are  $L_{i+1}$  filters corresponding to each output from the previous layer, a pooling operator is in high demand to reduce the computational complexity efficiently. In this paper, equation (17) is adopted to accomplish the required ‘pooling’ operation

$$Q_{d,k,g} = \sum_{\ell=1}^{L_{i+1}} Q_{d,k,g,\ell} = \sum_{\ell=1}^{L_{i+1}} 2^{\ell-1} S\{I_{d,k,g}^{out} \otimes W_\ell^d\}, \quad (17)$$

with each pixel being an integer in the range  $[0, 2^{L_{i+1}} - 1]$ . As a result, all the  $L_{i+1}$  images are combined into a single image, reducing the number of parameters and computation greatly. This procedure is depicted graphically in Figure. 6.

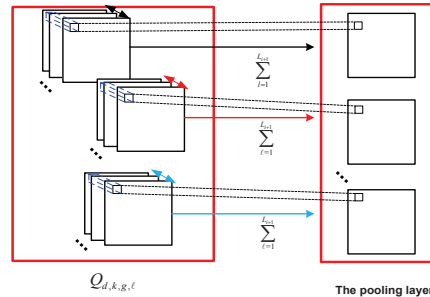


Figure 6. The pooling layer

### C. The information quality enhanced fully connected layer

The fully connected layer is utilized to connect every neuron in one layer to every neuron in another layer. In this paper, an information quality (IQ)–based fully connected layer is proposed as follows to accomplish this task.

Based on the previous subsection, each generated image  $Q_{d,k,g}$  is partitioned into  $A$  blocks. Different from the existing CCANet and related algorithms, information quality (IQ) instead of histogram is employed to generate the feature representation. As a non-linear descriptor, IQ has the potential to represent the intrinsic structure of input data/information more powerfully. The definition of IQ is given in (18)

$$H(p(t)) = -\log(p(t)), \quad (18)$$

TABLE I  
EXPERIMENTAL SETTINGS AND RESULTS ON THE ORL DATABASE

Methods	Patch Size	Layers	Filters	A Blocks	$\eta$	120 (Training)	200 (Training)	280 (Training)
CCANet	$3 \times 3$	2	$L_1 = L_2 = 8$	8	0.5	$83.89 \pm 4.72$	$94.55 \pm 2.10$	$97.83 \pm 1.63$
	$3 \times 3$	3	$L_1 = L_2 = L_3 = 8$	8	0.5	$86.64 \pm 3.89$	$94.70 \pm 1.97$	$97.92 \pm 0.90$
ODMTCNet	$3 \times 3$	2	$L_1 = L_2 = 8$	8	0.5	$85.96 \pm 0.04$	$95.45 \pm 2.03$	$98.25 \pm 1.07$
	$3 \times 3$	3	$L_1 = L_2 = L_3 = 8$	8	0.5	<b><math>87.89 \pm 3.90</math></b>	<b><math>95.80 \pm 1.83</math></b>	<b><math>98.50 \pm 1.23</math></b>

where  $p(t)$  is the prior probability of  $t$ .

Then, the IQ of the decimal values in each block is calculated and IQ values in all the  $A$  blocks with an overlapping ratio ( $\eta$ ) are transformed into one vector as  $H(Q_{d,k,g})$ . In ODMTCNet, the representation of the  $k$ th sample in the  $d$ th view is written in equation (19)

$$o_{k,d} = [H(Q_{d,k,1}), \dots, H(Q_{d,k,L_i})]^T \in R^{(2^{L(i+1)} L_i A)}. \quad (19)$$

The fully connected feature representation corresponding to the  $k$ th sample by integrating two different views is formulated in (20)

$$o_k = [o_{k,1}; o_{k,2}] \in R^{(2^{L(i+1)+1} L_i A)}. \quad (20)$$

The proposed feature representation architecture is illustrated in Figure. 7. This figure demonstrates that due to the combined strength of SML and DNN, not only are more discriminant feature maps generated, but abstract and robust semantics from large scale data sources are explored, yielding a high quality feature representation. Thus, by integrating data augmentation with more abstract and robust semantics, the proposed network works well on both small scale and large scale data sets.

#### D. Relation between the optimal performance and parameters

Having presented the basics in the proposed ODMTCNet, the relationship between the optimal performance and parameters (e.g., the number of convolutional filters in each layer) is presented below. According to the property of DCA in equation (7), the relation between the upper limit on the number of projected dimensions and the best solution is revealed as  $d \leq c$ , where  $d$  is the projected dimension associated with the global optimal performance and  $c$  is the number of classes. Based on the mathematical analysis and Figure 4, it is known that the output from convolution filters is equal to the projection in DCA space as shown in Figure 8.

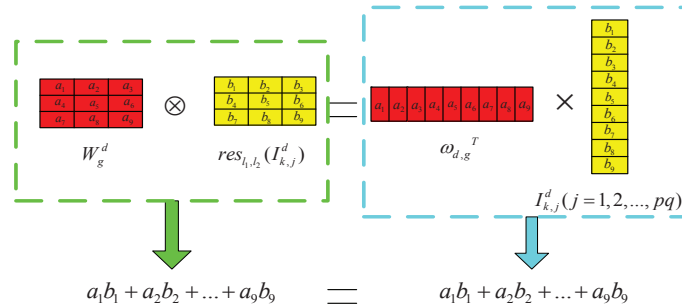


Figure 8. The convolutional output and projection in DCA

Since Figure 8 verifies that the output from convolution filters equals to the projection in DCA space, the outputs (e.g., feature maps) from the 2D convolutional filters also satisfy the property in equation (7). Therefore, the number of convolutional filters in each layer of ODMTCNet and the optimal performance can be predicted, leading to a discriminant representation. This is clearly a desirable and powerful feature of interpretable deep cascade networks.

The above analysis validates that since each convolutional layer in the ODMTCNet model generates discriminant knowledge representations, this work yields an interpretable DNN-based model on multi-view image feature representation. Note, as the discriminative representations are extracted according to an optimization function instead of a given/fixed loss function in each layer independently, the traditional BP algorithm is not required in the training process. By utilizing the designed discriminant multi-view tensor convolutional strategy, the proposed design leads to more distinct feature maps for rich data augmentation, leading to an effective solution to the small sample problem. In addition, due to utilization of the DNN-based cascade structure, more abstract and robust semantics are explored from large scale data sets. As a result, the proposed ODMTCNet model yields a high quality feature representation on image data sets of different scales. This key finding will be experimentally validated in the next section.

#### IV. EXPERIMENTAL RESULTS AND ANALYSIS

To validate the effectiveness of ODMTCNet, we conduct experiments on two different image-based tasks: face recognition and object recognition. To demonstrate the generality of the proposed network model, experiments are conducted on four data sets of different scale levels: small scale level, medium scale level and comparatively large scale level. Specifically, experiments are implemented on the Olivetti Research Lab (ORL) database (small level) [87], Facial Recognition Technology (FERET) database (small level) [88] for face recognition; the ETH-80 database (medium level) [89] and Caltech 256 (comparatively large level) database [90] for object recognition. In this work, we conducted experiments with different numbers of convolutional filters, and the best performance is reported. The ‘Training #’ in all tables denotes the number of training samples.

##### A. The ORL database

In this subsection, to examine the performance of ODMTCNet in face recognition, especially on a small scale database, we conduct experiments on the ORL database. In the ORL database, there are 40 subjects with 10 different samples for each person. The samples are captured under different conditions of illumination, facial expression, posing, etc. Some examples from the ORL are shown in Figure. 9.

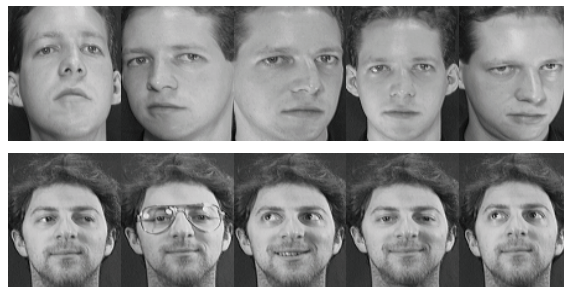


Figure. 9 Example images in the ORL database

During our experiments, the local binary patterns (LBP) [17] operation is performed on each sample to generate the second view data set for ODMTCNet. As a result, the original images and LBP maps are utilized jointly to accomplish the task of multi-view feature representation for face recognition as shown in Figure. 10.

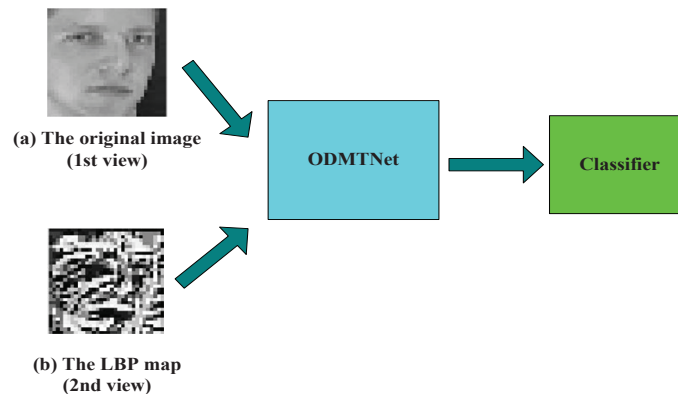


Figure 10. The diagram of ODMTCNet on the ORL database

All 400 samples in the ORL database are utilized, including the training subset and testing subset, respectively. In our experiments, we randomly select 120, 200 and 280 images to be training samples, while the remaining images are used as the testing samples. We run all experiments 10 times. To demonstrate the effectiveness of the ODMTCNet, the CCANet is also performed on the ORL database. The experimental settings and results (Average  $\pm$  Standard Deviation) are tabulated in TABLE 1. According to TABLE 1, it is observed that ODMTCNet always achieves better performance than that of CCANet with the same experimental settings. In addition, the average accuracy of ODMTCNet is improved with the number of training samples increasing. The comparison amongst state-of-the-art algorithms [8, 11, 18-33] is presented in TABLE 2, showing that ODMTCNet outperforms both statistical machine learning (SML) and DNN based algorithms. Moreover, it is seen that the number of all three filters  $L_i$  ( $i=1, 2, 3$ ) corresponding to the best average performance equals 8 (e.g.,  $L_1 = L_2 = L_3 = 8$ ) as shown in TABLE 1. This is substantially less than 40, the number of classes.

TABLE II  
COMPARISON WITH OTHER ALGORITHMS ON THE ORL DATABASE

Methods	Training #	Accuracy
MCPCADP [18]	200	91.25%
MDL [19]	200	92.15%
WLCRC [20]	200	92.69%
GLS [21]	200	93.33%
MSDL [22]	200	92.15%
GDLMP [23]	200	94.50%
CCA [24]	200	94.50%
MCCA [25]	200	94.50%
DSR [26]	200	95.00%
SOLDE-TR [27]	200	95.03%
CDPL [28]	200	95.42%
<b>ODMTCNet(<math>L_i &lt; 40</math>)</b>	200	<b>95.80%</b>
ANFIS-ABC [29]	280	96.00%
ESPP [30]	280	96.00%
CDM [31]	280	95.80%
CNN [8]	280	95.92%
PCANet [11]	280	96.28%
IKLDA+PNN [32]	280	96.35%
LiSSA [33]	280	97.51%
<b>ODMTCNet (<math>L_i &lt; 40</math>)</b>	280	<b>98.50%</b>

TABLE III  
EXPERIMENTAL SETTINGS AND RESULTS ON THE FERET DATABASE

Methods	Patch Size	Layers	Filters	A Blocks	$\eta$	Front-Left	Front-Right
CCANet	$3 \times 3$	2	$L_1 = L_2 = 8$	4	0.5	93.50	90.00
	$3 \times 3$	3	$L_1 = 14, L_2 = L_3 = 7$	8	0.5	95.50	91.50
ODMTCNet	$3 \times 3$	2	$L_1 = L_2 = 8$	4	0.5	96.50	92.00
	$3 \times 3$	3	$L_1 = 14, L_2 = L_3 = 7$	8	0.5	<b>96.50</b>	<b>93.00</b>

### B. The FERET database

In the FERET database, 600 samples of 200 subjects are chosen. Each subject provides three samples with a size of  $20 \times 20$  pixels according to three different poses (front, left and right) as shown in Figure. 11.



Figure. 11 Examples with different poses from the FERET database

Next, these samples are utilized to construct the first view data set and the twice wavelet transform [34] is performed on each sample in the first data set to generate the corresponding second data set. Moreover, two experimental settings are adopted, front-left and front-right. In the first one, the front samples are utilized for training and the others for testing. In the second, the front images are still adopted as train samples but the right samples are utilized for testing. Essentially, in this subsection, our task is to apply ODMTCNet to two-view single sample based face recognition, which is a challenging and popular research topic. Experimental settings and results on CCANet and ODMTCNet are tabulated in TABLE 3.

Furthermore, other two-view based methods [35-39] are applied to the above samples to verify the effectiveness of the proposed method. Since the two dimensional principal component analysis (2DPCA) [35] and two dimensional linear discriminant analysis (2DLDA) [36] algorithms are not able to explore the correlation between the two variable sets directly, they are applied to the first view data set only. Consequently, two dimensional CCA (2DCCA) [37], local two dimensional CCA (L2DCCA) [38] and complete discriminative tensor representation learning (CDTRL) [39] are performed on the two-view 2D data sets directly while samples are reshaped into one dimensional vectors for CCA [24]. Then, the recognition results are reported in TABLE 4.

TABLE IV  
RECOGNITION RESULTS WITH OTHER ALGORITHMS ON THE FERET DATASET

Method	Front-Left	Front-Right
2DPCA [35]	78.50%	76.50%
2DLDA [36]	71.50%	70.50%
CCA [24]	72.50%	68.50%
2DCCA-FFS1 [37]	80.50%	74.50%
2DCCA-FFS2 [37]	80.50%	74.00%
L2DCCA [38]	79.50%	75.00%
CDTRL [39]	83.00%	78.00%
<b>ODMTCNet (<math>L_i &lt; 200</math>)</b>	<b>96.50%</b>	<b>93.00%</b>

According to TABLE 4, it is observed that ODMTCNet outperforms the other two-view feature representation based methods, leading to greatly improved performance with a large margin. It validates the generality and effectiveness of the proposed ODMTCNet on the small scale data sets. Moreover, it is clearly seen in TABLE 3 that the number of filters associated with the optimal result equals 14 and 7 (e.g.,  $L_1 = 14, L_2 = L_3 = 7$ ). Again, this is far less than 200, the number of classes.

### C. The ETH-80 database

As a popular data set for multi-view feature representation studies, the ETH-80 database consists of 3280 color RGB object samples. All samples are divided into eight classes, including apples, cars, cows, cups, dogs, horses, pears and tomatoes. For each class, there are 410 images captured for 10 different objects and each object is presented by 41 images from a variety of angles. Some examples are shown in Figure. 12.

TABLE V  
EXPERIMENTAL SETTINGS AND RESULTS ON THE ETH-80 DATABASE

Methods	Patch Size	Layers	Filters	A Blocks	$\eta$	500 (Training)	1000 (Training)	1500 (Training)	1640 (Training)
CCANet	$7 \times 7$	2	$L_1 = L_2 = 8$	7	0.5	$86.05 \pm 0.89$	$91.97 \pm 0.61$	$93.62 \pm 0.61$	$93.98 \pm 0.21$
	$7 \times 7$	3	$L_1 = L_2 = 8, L_3 = 4$	7	0.5	$87.20 \pm 0.76$	$91.51 \pm 0.47$	$93.51 \pm 0.51$	$93.17 \pm 0.28$
ODMTCNet	$7 \times 7$	2	$L_1 = L_2 = 8$	7	0.5	<b><math>88.28 \pm 0.49</math></b>	<b><math>92.24 \pm 0.60</math></b>	<b><math>94.19 \pm 0.61</math></b>	<b><math>94.40 \pm 0.20</math></b>
	$7 \times 7$	3	$L_1 = L_2 = 8, L_3 = 4$	7	0.5	$88.16 \pm 0.91$	$92.19 \pm 0.79$	$93.60 \pm 0.27$	$93.69 \pm 0.12$



TABLE VI  
COMPARISON WITH OTHER STATE-OF-THE-ART ON THE ETH-80 DATABASE

Methods	Training #	Accuracy
LapMCC [40]	984	69.50%
HesMCC [41]	984	73.52%
<b>ODMTNet(<math>L_i &lt; 80</math>)</b>	500	<b>88.18%</b>
ALP-TMR [42]	1400	88.92%
<b>ODMTNet(<math>L_i &lt; 80</math>)</b>	1000	<b>92.24%</b>
Fine-tuned AlexNet [43]	1640	94.20%
SDNN [44]	1640	82.80%
MMFML-M3 [45]	1640	92.53%
MKDR-LR [46]	1640	91.20%
Kernel-LP [47]	1600	89.11%
CMCM [48]	1640	92.50%
JDRML [49]	1640	94.00%
MCCM-LE [50]	1640	93.30%
SML [51]	1640	94.02%
Sparsity+Intra-task [52]	1640	92.50%
TLRDA+PCA [53]	1640	92.00%
SSL-TR [54]	1640	93.40%
PLSRGStO [55]	1640	92.50%
SRC+DPC [56]	1640	94.00%
RMML-GM [57]	1640	90.25%
LRRTDR [58]	1640	92.00%
rBDLR [59]	2624	93.55%
PDOD+AOD+KNN [60]	3239	93.25%
<b>ODMTNet(<math>L_i &lt; 80</math>)</b>	1640	<b>94.40%</b>

TABLE VII  
PERFORMANCE OF FC6 AND FC7 ON THE CALTECH256 DATABASE

Feature	Recognition Accuracy
<b>fc6</b>	58.22%
<b>fc7</b>	59.81%

samples are used in training. Note, the number of filters  $L_i$  ( $i=1, 2, 3$ ) corresponding to the best performance is 8 and 4 (e.g.,  $L_1 = L_2 = 8, L_3 = 4$ ) shown in TABLE 8. This is much less than the number of classes 257 in the Caltech 256 database.

### E. Discussions

The presented mathematical analysis and experimental validation clearly demonstrate that the proposed ODMTCNet operates well on image data sets of different scale levels, outperforming all the comparing algorithms as shown in Tables 2, 4, 6 and 9. Furthermore, the following desirable properties of ODMTCNet are observed:

- The network is able to take image features in all popular formats as input: pixel values in ORL and ETH-80, hand-crafted features in FERET and DNN features in Caltech 256.
- The number of filters ( $L_i$ ) leading to the best accuracy is much lower than the number of classes, validating the desirable relation presented in Section 3.4. In fact, the number of convolutional parameters corresponding to the filters is on the scale of several hundreds (as shown in Tables 1, 3, 5, and 8), stunningly different from that of mainstream DNNs (on the scale of tens of millions up to several billions).

TABLE VIII  
EXPERIMENTAL SETTINGS AND RESULTS ON THE CALTECH 256 DATABASE

Methods	Patch Size	Layers	Filters	A Blocks	$\eta$	30/class $\times$ 257=7710 (Training)	60/class $\times$ 257=15420 (Training)
CCANet	5 $\times$ 5	2	$L_1 = L_2 = 8$	8	0.5	84.81 $\pm$ 1.00	87.20 $\pm$ 0.40
	5 $\times$ 5	3	$L_1 = L_2 = 8, L_3 = 4$	8	0.5	85.07 $\pm$ 0.44	87.82 $\pm$ 0.33
ODMTCNet	5 $\times$ 5	2	$L_1 = L_2 = 8$	8	0.5	86.27 $\pm$ 0.31	87.25 $\pm$ 0.31
	5 $\times$ 5	3	$L_1 = L_2 = 8, L_3 = 4$	8	0.5	<b>86.33 <math>\pm</math> 0.26</b>	<b>88.34 <math>\pm</math> 0.35</b>

With drastically smaller number of convolutional parameters, fit for training on CPU scale processors, the studies reported in this paper potentially open up a new and more accessible path for the promotion of interpretable machine learning (I-ML) in both academic research and practical applications.

## V. CONCLUSIONS

In this paper, an optimal discriminant multi-view tensor convolutional network (ODMTCNet) is proposed for deep level multi-view feature representation. By integrating the SML principles with DNN architecture, the parameters of convolutional layers are determined by an analytical solution instead of the traditional BP algorithm. Hence, the proposed ODMTCNet forms a foundational platform for an interpretable machine learning model which generates feature representation of high quality from original multi-view data sources. Furthermore, the representation effectively addresses the overfitting problem when there is no sufficient data available in training. The desirable properties of ODMTCNet are validated by numerous application examples with image data sets of different scales. To conclude this paper, it is worth noting that the number of convolutional layers corresponding to the optimal performance in ODMTCNet is smaller than or equals to 3 in all the four evaluation examples, approaching the bound predicted in Kolmogorov Superposition Theorem [93-94] in neural network-based representation.

## REFERENCES

- [1] Y. Bengio, A. Courville, and P. Vincent. "Representation learning: A review and new perspectives." *IEEE transactions on pattern analysis and machine intelligence*, vol. 35, no. 8, pp. 1798–1828, 2013.
- [2] X. Jia, X.Y. Jing, X. Zhu, S. Chen, B. Du, Z. Cai, Z. He, and D. Yue. "Semi-supervised Multi-view Deep Discriminant Representation Learning." *IEEE Transactions on Pattern Analysis and Machine Intelligence (early access)*, 2020.
- [3] S.M. Kazemi, R. Goel, K. Jain, I. Kobyzev, A. Sethi, P. Forsyth, and P. Poupart. "Representation Learning for Dynamic Graphs: A Survey." *Journal of Machine Learning Research*, vol. 21, no. 70, pp. 1–73, 2020.
- [4] X. Yang, W. Liu, D. Tao, and J. Cheng. "Canonical correlation analysis networks for two-view image recognition." *Information Sciences*, vol. 385, pp. 338–352, 2017.
- [5] X. He, S. Yan, Y. Hu, P. Niyogi, and H.J. Zhang. "Face recognition using laplacianfaces." *IEEE transactions on pattern analysis and machine intelligence*, vol. 27, no. 3, pp. 328–340, 2005.
- [6] C. Zhang, H. Fu, J. Wang, W. Li, X. Cao, and Q. Hu. "Tensorized Multi-view Subspace Representation Learning." *International Journal of Computer Vision*, vol. 128, no. 8, pp. 1–18, 2020.
- [7] Y. Sun, Z. Zhang, W. Jiang, Z. Zhang, L. Zhang, S. Yan, and M. Wang. "Discriminative local sparse representation by robust adaptive dictionary pair learning." *IEEE Transactions on Neural Networks and Learning Systems (early access)*, 2020.
- [8] A. Krizhevsky, I. Sutskever, and G. E. Hinton. "ImageNet classification with deep convolutional neural network." *In Advances in neural information processing systems*, pp. 1097–1105, 2012.
- [9] Y. Liu, J. Han, Q. Zhang, and C. Shan. "Deep salient object detection with contextual information guidance." *IEEE Transactions on Image Processing*, vol. 29, pp. 360–374, 2019.
- [10] F. Huang, C. Jin, Y. Zhang, K. Weng, T. Zhang, and W. Fan. "Sketch-based image retrieval with deep visual semantic descriptor." *Pattern Recognition*, vol. 76, pp. 537–548, 2018.
- [11] T.H. Chan, K. Jia, S. Gao, J. Lu, Z. Zeng and Y. Ma. "PCANet: A simple deep learning baseline for image classification?" *IEEE Transactions on Image Processing*, vol. 24, no. 12, pp. 5017–5032, 2015.
- [12] C.J. Ng, and A.B.J. Teoh. "DCTNet: A simple learning-free approach for face recognition." *2015 Asia-Pacific Signal and Information Processing Association Annual Summit and Conference (APSIPA)*, pp. 761–768, 2015.
- [13] X.T. Yuan, X. Liu, and S. Yan. "Visual classification with multitask joint sparse representation." *IEEE Trans. Image Processing*, vol. 21, no. 10, pp. 4349–4360, 2012.
- [14] B.B. Gatto, and E.M. Dos Santos. "Discriminative canonical correlation analysis network for image classification." *2017 IEEE International Conference on Image Processing (ICIP)*, pp. 4487–4491, 2017.
- [15] L. Gao, L. Qi, E. Chen, and L. Guan. "Discriminative multiple canonical correlation analysis for information fusion." *IEEE Transactions on Image Processing*, vol. 27, no. 4, pp. 1951–1965, 2018.
- [16] S. Lawrence, C.L. Giles, A.C. Tsoi, and A.D. Back. "Face recognition: A convolutional neural-network approach." *IEEE transactions on neural networks*, vol. 8, no. 1, pp. 98–113, 1997.
- [17] B. Yang, and S. Chen. "A comparative study on local binary pattern (LBP) based face recognition: LBP histogram versus LBP image." *Neurocomputing*, vol. 120, pp. 365–379, 2013.
- [18] H. Chen, J. Li, J. Gao, Y. Sun, Y. Hu, and B. Yin. "Maximally Correlated Principal Component Analysis Based on Deep Parameterization Learning." *ACM Transactions on Knowledge Discovery from Data (TKDD)*, vol. 13, no. 4, pp. 1–17, 2019.
- [19] X. Luo, Y. Xu, and J. Yang. "Multi-resolution dictionary learning for face recognition." *Pattern Recognition*, vol. 93, pp. 283–292, 2019.
- [20] X. Dong, H. Zhang, L. Zhu, W. Wan, Z. Wang, Q. Wang, P. Guo, H. Ji, and J. Sun. "Weighted locality collaborative representation based on sparse subspace." *Journal of Visual Communication and Image Representation*, vol. 58, pp. 187–194, 2019.
- [21] X. Shen, S. Liu, B. Bao, C. Pan, Z. Zha, and J. Fan. "A generalized least-squares approach regularized with graph embedding for dimensionality reduction." *Pattern Recognition*, vol. 98, pp. 1–10, 2020.
- [22] X. Luo, Y. Xu, and J. Yang. "Multi-resolution dictionary learning for face recognition." *Pattern Recognition*, vol. 93, pp. 283–292, 2019.

TABLE IX  
 RECOGNITION ACCURACY WITH OTHER METHODS ON THE CALTECH 256

Methods	Training #	Accuracy
CMFA-SR [62]	7710	71.44%
DGFLP [63]	7710	69.17%
BMDDL [65]	7710	59.30%
LLKc [66]	7710	72.09%
ISC-LG [67]	7710	50.62%
BLF-FV [68]	7710	51.42%
OCB-FV [69]	7710	53.15%
LLC-SVM [70]	7710	34.50%
SWSS-VGG [71]	7710	73.56%
ResNet152 [72]	7710	78.00%
ResFeats152 [73]	7710	79.50%
MVLS [74]	7710	84.23%
NR [75]	7710	84.40%
TransTailor [64]	7710	85.30%
Hybrid1365-VGG [76]	7710	76.04%
LMCCA [77]	7710	76.52%
PtR [78]	7710	84.50%
DMCCA [15]	7710	80.32%
Autuencoder-DenseNet-121 [95]	7710	80.60%
HMML [79]	12850	64.06%
DCS [80]	13770	64.18%
<b>ODMTCNet (<math>L_i &lt; 257</math>)</b>	7710	<b>86.33%</b>
CMFA-SR [62]	15420	76.31%
SMNN+VGG-19 [81]	15420	81.90%
SMNN+Resnet152 [81]	15420	82.30%
SMNN+Xception [81]	15420	84.70%
LLKc [66]	15420	75.36%
ISC-LG [67]	15420	55.76%
OCB-FV [69]	15420	59.03%
LLC-SVM [70]	15420	40.10%
SWSS-VGG [71]	15420	76.25%
ResNet152 [72]	15420	81.90%
ResFeats152 [73]	15420	82.10%
NAC [82]	15420	84.10%
Joint fine-tuning [83]	15420	83.80%
DFG [80]	15420	87.09%
<b>ODMTCNet (<math>L_i &lt; 257</math>)</b>	15420	<b>88.34%</b>

- [23] Ming-Hua Wan, and Zhi-Hui Lai. "Generalized Discriminant Local Median Preserving Projections (GDLMP) for Face Recognition." *Neural Processing Letters*, pp. 1–13, 2018.
- [24] Q.S. Sun, S.G. Zeng, Y. Liu, P.A. Heng, and D.S. Xia. "A new method of feature fusion and its application in image recognition." *Pattern Recognition*, vol. 38, no. 12, pp. 2437–2448, 2005.
- [25] Y. Li, T. Adali, W. Wang, and V.D. Calhoun. "Joint blind source separation by multiset canonical correlation analysis." *IEEE Transactions on Signal Processing*, vol. 57, no. 10, pp. 3918–3929, 2009.
- [26] Y. Xu, Z. Zhong, J. Yang, J. You and David Zhang. "A New Discriminative Sparse Representation Method for Robust Face Recognition via  $l_1$  Regularization." *IEEE transactions on neural networks and learning systems*, vol. 28, no. 10, pp. 2233–2241, 2017.
- [27] X. Yang, G. Liu, Q. Yu, and R. Wang. "Stable and orthogonal local discriminant embedding using trace ratio criterion for dimensionality reduction."

- Multimedia Tools and Applications*, vol. 77, no. 3, pp. 3071–3081, 2018.
- [28] M. Meng, M. Lan, J. Yu, J. Wu, and D. Tao. “Constrained Discriminative Projection Learning for Image Classification.” *IEEE Transactions on Image Processing*, vol. 29, pp. 186–198, 2019.
- [29] M.R. Rejeesh. “Interest point based face recognition using adaptive neuro fuzzy inference system.” *Multimedia Tools and Applications*, vol. 78, no. 16, pp. 22691–22710, 2019.
- [30] W. Wei, H. Dai, and W. Liang. “Exponential sparsity preserving projection with applications to image recognition.” *Pattern Recognition*, vol. 104, pp. 1–11, 2020.
- [31] C. Liu, J. Wang, S. Duan, and Y. Xu. “Combining dissimilarity measures for image classification.” *Pattern Recognition Letters*, vol. 128, pp. 536–543, 2019.
- [32] A. Ouyang, Y. Liu, S. Pei, X. Peng, M. He, and Q. Wang. “A hybrid improved kernel LDA and PNN algorithm for efficient face recognition.” *Neurocomputing*, vol. 393, pp. 214–222, 2019.
- [33] T. Wang, W.W. Ng, M. Pelillo and S. Kwong. “LiSSA: localized stochastic sensitive autoencoders.” *IEEE Transactions on Cybernetics (Early Access)*, 2019.
- [34] X. Gao, S. Niu, and Q. Sun. “Two-directional two-dimensional kernel canonical correlation analysis.” *IEEE Signal Process. Lett.*, vol. 26, no. 11, pp. 1578–1582, 2019.
- [35] J. Yang, D. Zhang, A. F. Frangi, and J. Yang. “Two-dimensional PCA: A new approach to appearance-based face representation and recognition.” *IEEE Trans. Pattern Anal. Mach. Intell.*, vol. 26, no. 1, pp. 131–137, 2004.
- [36] J. Ye, R. Janardan, and Q. Li. “Two-dimensional linear discriminant analysis.” *Proc. Adv. Neural Inf. Process. Syst.*, pp. 1569–1576, 2005.
- [37] S.H. Lee and S. Choi. “Two-dimensional canonical correlation analysis.” *IEEE Signal Process. Lett.*, vol. 14, no. 10, pp. 735–738, 2007.
- [38] H.X. Wang. “Local two-dimensional canonical correlation analysis.” *IEEE Signal Process. Lett.*, vol. 17, no. 11, pp. 921–924, 2010.
- [39] L. Gao, and L. Guan. “A Complete Discriminative Tensor Representation Learning for Two-Dimensional Correlation Analysis.” *IEEE Signal Processing Letters*, vol. 27, pp. 1894–1898, 2020.
- [40] Y. Yuan, Y. Li, X. Shen, Q. Sun, and J. Yang. “Laplacian multiset canonical correlations for multiview feature extraction and image recognition.” *Multimedia Tools and Applications*, vol. 76, no. 1, pp. 731–755, 2017.
- [41] W. Liu, X. Yang, D. Tao, J. Cheng, and Y. Tang. “Multiview dimension reduction via Hessian multiset canonical correlations.” *Information Fusion*, vol. 41, pp. 119–128, 2018.
- [42] H. Zhang, Z. Zhang, M. Zhao, Q. Ye, M. Zhang, and M. Wang. “Robust triple-matrix-recovery-based auto-weighted label propagation for classification.” *IEEE Transactions on Neural Networks and Learning Systems (Early Access)*, 2020.
- [43] X. Wu, Y. Wang, H. Tang, and R. Yan. “A structure–time parallel implementation of spike-based deep learning.” *Neural Networks*, vol. 113, pp. 72–78, 2019.
- [44] S.R. Kheradpisheh, M. Ganjtabesh, S.J. Thorpe, and T. Masquelier. “STDP-based spiking deep convolutional neural networks for object recognition.” *Neural Networks*, vol. 99, pp. 56–67, 2018.
- [45] X. Gao, Q. Sun, H. Xu, D. Wei, and J. Gao. “Multi-model fusion metric learning for image set classification.” *Knowledge-Based Systems*, vol. 164, pp. 253–264, 2019.
- [46] W. Yan, H. Sun, Q. Sun, Z. Zheng, X. Gao, Q. Zhang, and Z. Ren. “Multiple kernel dimensionality reduction based on collaborative representation for set oriented image classification.” *Expert Systems with Applications*, vol. 137, pp. 380–391, 2019.
- [47] Z. Zhang, L. Jia, M. Zhao, G. Liu, M. Wang, and S. Yan. “Kernel-induced label propagation by mapping for semi-supervised classification.” *IEEE Transactions on Big Data*, vol. 5, no. 2, pp. 148–165, 2018.
- [48] N. Sogi, T. Nakayama, and K. Fukui. “A method based on convex cone model for image-set classification with cnn features.” *International Joint Conference on Neural Networks (IJCNN)*, pp. 1–8, 2018.
- [49] W. Yan, Q. Sun, H. Sun, and Y. Li. “Joint dimensionality reduction and metric learning for image set classification.” *Information Sciences*, vol. 516, pp. 109–124, 2020.
- [50] K. Zhao, A. Wiliem, S. Chen, and B.C. Lovell. “Convex class model on symmetric positive definite manifolds.” *Image and Vision Computing*, vol. 87, pp. 57–67, 2019.
- [51] E. Vural, and C. Guillemot. “A study of the classification of low-dimensional data with supervised manifold learning.” *Journal of Machine Learning Research*, vol. 18, no. 1, pp. 5741–5795, 2017.
- [52] D. Liu, L. Liu, Y. Tie, and L. Qi. “Multi-task image set classification via joint representation with class-level sparsity and intra-task low-rankness.” *Pattern Recognition Letters*, vol. 132, pp. 99–105, 2020.
- [53] J. Zhang, Z. Li, P. Jing, Y. Liu, and Y. Su. “Tensor-driven low-rank discriminant analysis for image set classification.” *Multimedia Tools and Applications*, vol. 78, no. 4, pp. 4001–4020, 2019.
- [54] W. Yan, Q. Sun, H. Sun, and Y. Li. “Semi-Supervised Learning Framework Based on Statistical Analysis for Image Set Classification.” *Pattern Recognition*, vol. 107, pp. 1–13, 2020.
- [55] H. Chen, Y. Sun, J. Gao, Y. Hu, and B. Yin. “Solving partial least squares regression via manifold optimization approaches.” *IEEE transactions on neural networks and learning systems*, vol. 30, no. 2, pp. 588–600, 2018.
- [56] K. Sharma, and R. Rameshan. “Image Set Classification Using a Distance-Based Kernel Over Affine Grassmann Manifold.” *IEEE Transactions on Neural Networks and Learning Systems (Early Access)*, 2020.
- [57] N. Sogi, L.S. Souza, B.B. Gatto, and K. Fukui. “Metric Learning With A-Based Scalar Product for Image-Set Recognition.” *IEEE Conference on Computer Vision and Pattern Recognition Workshops*, pp. 850–851, 2020.
- [58] P. Jing, Y. Su, Z. Li, J. Liu, and L. Nie. “Low-rank regularized tensor discriminant representation for image set classification.” *Signal Processing*, vol. 156, pp. 62–70, 2019.
- [59] Z. Zhang, J. Ren, S. Li, R. Hong, Z. Zha, and M. Wang. “Robust subspace discovery by block-diagonal adaptive locality-constrained representation.” *27th ACM international conference on multimedia*, pp. 1569–1577, 2019.
- [60] A. Elboushaki, R. Hannane, K. Afdel, and L. Koutti. “A robust approach for object matching and classification using Partial Dominant Orientation Descriptor.” *Pattern Recognition*, vol. 64, pp. 168–186, 2017.
- [61] K. Simonyan, A. Zisserman. “Very deep convolutional networks for large-scale image recognition.” *2015 International Conference on Learning Representations*, pp. 1–14, 2015.
- [62] A. Puthenputhussery, Q. F. Liu, and C. J. Liu. “A sparse representation model using the complete marginal fisher analysis framework and its applications to visual recognition.” *IEEE Transactions on Multimedia*, vol. 19, no. 8, pp. 1757–1770, 2017.
- [63] G. F. Lin, K. Liao, B. Sun, Y. Chen, and F. Zhao. “Dynamic graph fusion label propagation for semi-supervised multi-modality classification.” *Pattern Recognition*, vol. 68, pp. 14–23, 2017.
- [64] B. Liu, Y. Cai, Y. Guo, and X. Chen. “TransTailor: Pruning the Pre-trained Model for Improved Transfer Learning.” *2021 AAAI Conference on Artificial Intelligence*, vol. 35, no. 10, pp. 8627–8634, 2021.
- [65] P. Zhou, C. Zhang, and Z. C. Lin. “Bilevel model-based discriminative dictionary learning for recognition.” *IEEE Transactions on Image Processing*, vol. 26, no. 3, pp. 1173–1187, 2017.
- [66] Q. F. Liu, and C. Liu. “A novel locally linear KNN method with applications to visual recognition.” *IEEE transactions on neural networks and learning systems*, vol. 28, no. 9, pp. 2010–2021, 2017.

- [67] C. J. Zhang, J. Cheng, C. Li, and Q. Tian. "Image-specific classification with local and global discriminations." *IEEE transactions on neural networks and learning systems*, vol. 29, no. 9, 4479–4486, 2018.
- [68] C. J. Zhang, J. Sang, G. B. Zhu, and Q. Tian. "Bundled local features for image representation." *IEEE Transactions on Circuits and Systems for Video Technology*, vol. 28, no. 8, 1719–1726, 2018.
- [69] C. Zhang, G. Zhu, C. Liang, Y. Zhang, Q. Huang, and Q. Tian. "Image class prediction by joint object, context, and background modeling." *IEEE Transactions on Circuits and Systems for Video Technology*, vol. 28, no. 2, pp. 428–438, 2018.
- [70] W. Luo, J. Li, J. Yang, W. Xu, and J. Zhang. "Convolutional sparse autoencoders for image classification." *IEEE transactions on neural networks and learning systems*, vol. 29, no. 7, 3289–3294, 2018.
- [71] C. J. zhang, J. Cheng, and Q. Tian. "Structured weak semantic space construction for visual categorization." *IEEE transactions on neural networks and learning systems*, vol. 29, no. 8, pp. 3442–3451, 2018.
- [72] K. M. He, X. Zhang, S. Ren, and J. Sun. "Deep residual learning for image recognition." In *Proceedings of the IEEE conference on computer vision and pattern recognition*, pp. 770–778, 2016.
- [73] A. Mahmood, M. Bennamoun, S. An and F. Sohel. "Resfeats: Residual network based features for image classification." *2017 IEEE International Conference on In Image Processing (ICIP)*, pp. 1597–1601, 2017.
- [74] C. Zhang, J. Cheng, and Q. Tian. "Multiview label sharing for visual representations and classifications." *IEEE Transactions on Multimedia*, vol. 20, no. 4, pp. 903–913, 2017.
- [75] J. Xu, W. An, L. Zhang, and D. Zhang. "Sparse, collaborative, or nonnegative representation: which helps pattern classification?." *Pattern Recognition*, vol. 88, pp. 679–688, 2019.
- [76] B. Zhou, A. Lapedriza, A. Khosla, A. Oliva, and A. Torralba. "Places: A 10 million image database for scene recognition." *IEEE transactions on pattern analysis and machine intelligence*, vol. 40, no. 6, pp. 1452–1464, 2018.
- [77] L. Gao, R. Zhang, L. Qi, E. Chen, and L. Guan. "The labeled multiple canonical correlation analysis for information fusion." *IEEE Transactions on Multimedia*, vol. 21, no. 2, pp. 375–387, 2019.
- [78] Y. Zhong, and A. Maki. "Regularizing CNN transfer learning with randomised regression." *2020 IEEE/CVF Conference on Computer Vision and Pattern Recognition*, pp. 13637–13646, 2020.
- [79] Y. Zheng, J. P. Fan, J. Zhang, and X. Gao. "Hierarchical learning of multi-task sparse metrics for large scale image classification." *Pattern Recognition*, vol. 67, pp. 97–109, 2017.
- [80] S. Suh, P. Lukowicz, and Y. Lee. "Discriminative feature generation for classification of imbalanced data." *Pattern Recognition*, vol. 122, pp. 1–13, 2022.
- [81] D. Wang, and K. Mao. "Learning Semantic Text Features for Web Text-Aided Image Classification." *IEEE Transactions on Multimedia*, vol. 21, no. 12, pp. 2985–2996, 2019.
- [82] M. Simon, and E. Rodner. "Neural activation constellations: Unsupervised part model discovery with convolutional networks." *IEEE international conference on computer vision*, pp. 1143–1151, 2015.
- [83] W. Ge, and Y. Yu. "Borrowing treasures from the wealthy: Deep transfer learning through selective joint fine-tuning." *IEEE conference on computer vision and pattern recognition*, pp. 1086–1095, 2017.
- [84] M.M. Najafabadi, F. Villanustre, T.M. Khoshgoftaar, N. Seliya, R. Wald, and E. Muharemagic. "Deep learning applications and challenges in big data analytics." *Journal of big data*, vol. 2, no. 1, pp. 1–21, 2015.
- [85] L. Zhou, S. Pan, J. Wang, and A.V. Vasilakos. "Machine learning on big data: Opportunities and challenges." *Neurocomputing*, vol. 237, pp. 350–361, 2017.
- [86] G. Zhong, L. Wang, X. Ling, and J. Dong. "An overview on data representation learning: From traditional feature learning to recent deep learning." *The Journal of Finance and Data Science*, vol. 2, no. 4, pp. 265–278, 2016.
- [87] F.S. Samaria, A.C. Harter, "Parameterisation of a stochastic model for human face identification." *Proceedings of 1994 IEEE workshop on applications of computer vision*, IEEE, pp. 138–142, 1994.
- [88] P. Phillips, H.M. Jonathon, S.A. Rizvi, and P.J. Rauss. "The FERET evaluation methodology for face-recognition algorithms." *IEEE Transactions on pattern analysis and machine intelligence*, vol. 22, no. 10, pp. 1090–1104, 2000.
- [89] B. Leibe, and B. Schiele. "Analyzing appearance and contour based methods for object categorization." *2003 IEEE Computer Society Conference on Computer Vision and Pattern Recognition*, pp. II–409, 2003.
- [90] G. Griffin, A. Holub, and P. Perona. "Caltech-256 object category dataset." 2007.
- [91] Q. Zhang, Y.N. Wu, and S.C. Zhu. "Interpretable convolutional neural networks." *2018 IEEE Conference on Computer Vision and Pattern Recognition*, pp. 8827–8836, 2018.
- [92] C-C.J. Kuo, M. Zhang, S. Li, J. Duan, and Y. Chen. "Interpretable convolutional neural networks via feedforward design." *Journal of Visual Communication and Image Representation*, vol. 60, pp. 346–359, 2019.
- [93] A. Kolmogorov. "On the representation of continuous functions of several variables by superpositions of continuous functions of a smaller number of variables." *Proceedings of the USSR Academy of Sciences*, vol. 108, pp. 179–182, 1956.
- [94] V.I. Arnold. "On functions of three variables." *Doklady Akademii Nauk*, vol. 114, no. 4, pp. 679–681, 1957.
- [95] X. Feng, Q. Wu, Y. Yang, and L. Cao. "An Autoencoder-based Data Augmentation Strategy for Generalization Improvement of DCNNs." *Neurocomputing*, vol. 402, pp. 283–297, 2020.